

## $\beta_3$ Adrenergic Stimulation Restores Nitric Oxide/Redox Balance and Enhances Endothelial Function in Hyperglycemia

Keyvan Karimi Galougahi, MD, PhD; Chia-Chi Liu, PhD; Alvaro Garcia, BSc, PhD; Carmine Gentile, PharmD, PhD; Natasha A. Fry, BSc, PhD; Elisha J. Hamilton, PhD; Clare L. Hawkins, BSc, DPhil; Gemma A. Figtree, MBBS, DPhil

**Background**—Perturbed balance between NO and  $O_2^{\bullet-}$  (ie, NO/redox imbalance) is central in the pathobiology of diabetes-induced vascular dysfunction. We examined whether stimulation of  $\beta_3$  adrenergic receptors ( $\beta_3$  ARs), coupled to endothelial nitric oxide synthase (eNOS) activation, would re-establish NO/redox balance, relieve oxidative inhibition of the membrane proteins eNOS and  $Na^+-K^+$  (NK) pump, and improve vascular function in a new animal model of hyperglycemia.

**Methods and Results**—We established hyperglycemia in male White New Zealand rabbits by infusion of S961, a competitive high-affinity peptide inhibitor of the insulin receptor. Hyperglycemia impaired endothelium-dependent vasorelaxation by “uncoupling” of eNOS via glutathionylation (eNOS-GSS) that was dependent on NADPH oxidase activity. Accordingly, NO levels were lower while  $O_2^{\bullet-}$  levels were higher in hyperglycemic rabbits. Infusion of the  $\beta_3$  AR agonist CL316243 (CL) decreased eNOS-GSS, reduced  $O_2^{\bullet-}$ , restored NO levels, and improved endothelium-dependent relaxation. CL decreased hyperglycemia-induced NADPH oxidase activation as suggested by co-immunoprecipitation experiments, and it increased eNOS co-immunoprecipitation with glutaredoxin-1, which may reflect promotion of eNOS de-glutathionylation by CL. Moreover, CL reversed hyperglycemia-induced glutathionylation of the  $\beta_1$  NK pump subunit that causes NK pump inhibition, and improved  $K^+$ -induced vasorelaxation that reflects enhancement in NK pump activity. Lastly, eNOS-GSS was higher in vessels of diabetic patients and was reduced by CL, suggesting potential significance of the experimental findings in human diabetes.

**Conclusions**— $\beta_3$  AR activation restored NO/redox balance and improved endothelial function in hyperglycemia.  $\beta_3$  AR agonists may confer protection against diabetes-induced vascular dysfunction. (*J Am Heart Assoc.* 2016;5:e002824 doi: 10.1161/JAHA.115.002824)

**Key Words:**  $\beta_3$  adrenergic receptors • endothelial dysfunction • endothelial nitric oxide synthase • hyperglycemia • oxidative stress

Elevated levels of reactive oxygen species (ROS), or “oxidative stress” and decreased NO levels are central pathobiological features of vascular dysfunction in diabetes.<sup>1</sup> At low levels, ROS play an important role in physiological cell

signaling.<sup>2,3</sup> Within the signaling microdomains in membrane lipid rafts/caveolae, the levels of ROS are kept in a tight balance with NO for optimal signaling, in what is known as “NO/redox balance.”<sup>3</sup> The NO/redox balance is structurally based on co-localization of NADPH oxidase, the major source of ROS in the membrane, with endothelial NO synthase (eNOS) and their signaling interaction.<sup>3</sup> In diabetes, excessive activation of the oxidase and a switch in the function of eNOS from NO- to ROS generation (ie, eNOS “uncoupling”) causes disruption of this balance, resulting in adverse effects on cellular homeostasis and vascular function.<sup>2,3</sup>

Despite the established role of ROS in diabetes-induced vascular dysfunction, general antioxidants are clinically ineffective.<sup>2</sup> Even if general antioxidants are successfully delivered to the membrane signalosomes, a feat that is yet to be established,<sup>4</sup> and they scavenge ROS on a one-to-one basis, they have no effects on sources of ROS; whereas diabetes-induced NADPH oxidase-derived ROS generation is a continuous process.<sup>1</sup> In physiological signaling, antioxidants

From the North Shore Heart Research Group, Kolling Institute (K.K.G., C.-C.L., A.G., N.A.F., E.J.H., G.A.F.) and School of Medicine (C.G.), University of Sydney, Australia; University of Sydney Medical School Foundation, Sydney, Australia (K.K.G.); Columbia University Medical Center, New York, NY (K.K.G.); Department of Cardiology, Royal North Shore Hospital, Sydney, Australia (G.A.F.); Heart Research Institute, Sydney, Australia (C.G., C.L.H.).

**Correspondence to:** Gemma A. Figtree, MBBS, DPhil, North Shore Heart Research Group, Kolling Institute of Medical Research, Royal North Shore Hospital, St Leonards, NSW 2065, Australia. E-mail: gemma.figtree@sydney.edu.au

Received October 28, 2015; accepted January 7, 2016.

© 2016 The Authors. Published on behalf of the American Heart Association, Inc., by Wiley Blackwell. This is an open access article under the terms of the Creative Commons Attribution-NonCommercial License, which permits use, distribution and reproduction in any medium, provided the original work is properly cited and is not used for commercial purposes.

need to achieve “controlled” generation rather than complete suppression of ROS. In contrast to nonspecific antioxidants, disruption of the renin–angiotensin system in diabetes by angiotensin-converting enzyme inhibitors or angiotensin receptor blockers protects against the diabetes-induced vascular dysfunction.<sup>2</sup> Angiotensin II (Ang II) receptors are co-localized with NADPH oxidase and eNOS,<sup>5</sup> and inhibition of Ang II receptor–coupled signaling re-establishes NO/redox balance by decreasing NADPH oxidase–mediated ROS production<sup>2</sup> and by restoring eNOS function.<sup>6,7</sup>

Due to a paucity of therapies protective against vascular complications of diabetes besides angiotensin-converting enzyme inhibitors/angiotensin receptor blockers, we sought to determine whether agents that modulate adrenergic signaling via  $\beta_3$  adrenergic receptors ( $\beta_3$  ARs) have effects on redox pathways and vascular function in hyperglycemic state.  $\beta_3$  ARs are expressed in endothelial cells<sup>8</sup> and enriched in the caveolae<sup>9</sup> and their stimulation is coupled to eNOS activation and NO release.<sup>10,11</sup> We have previously shown that  $\beta_3$  AR stimulation reverses oxidative inhibition of the cardiac  $\text{Na}^+\text{-K}^+$  pump,<sup>10,11</sup> a biomolecule also enriched in the caveolae.<sup>12</sup> This effect was mediated by a decrease in glutathionylation of the pump's  $\beta_1$  subunit.<sup>10</sup> Glutathionylation, which involves formation of a reversible disulphide bond between glutathione and reactive cysteines on proteins with significant structural and functional consequences, is increasingly recognized in physiological and pathophysiological cell signaling.<sup>13</sup> Of direct relevance to our objective, glutathionylation also mediates eNOS uncoupling in endothelial cells under oxidative stress.<sup>14</sup> In contrast to uncoupling by depletion of the cofactor tetrahydrobiopterin ( $\text{BH}_4$ ), which leads to  $\text{O}_2^{\bullet-}$  generation in the oxidase domain of the enzyme instead of NO synthesis, uncoupling by glutathionylation of 2 highly conserved cysteine residues of eNOS leads to  $\text{O}_2^{\bullet-}$  generation in the reductase domain and abolishment of NO production.<sup>14</sup> These seemingly distinct mechanisms of eNOS uncoupling have recently been shown to interact, with one mechanism inducing uncoupling by the other in an integrated manner.<sup>15</sup>

To study the effects of  $\beta_3$  AR agonism in diabetes, we established and characterized a novel model of hyperglycemia because we found that the widely used diabetogenic agents such as streptozotocin (STZ) and alloxan, which induce type 1 diabetes, have direct and confounding effects on glutathionylation levels. The prevalence of type 2 diabetes is substantially higher than type 1, driven by the epidemics of obesity and insulin resistance,<sup>16</sup> and is alarmingly on the rise with vascular pathophysiology being the major cause of morbidity and mortality. Since both disruption in insulin signaling<sup>17</sup> and hyperglycemia<sup>16</sup> are key pathophysiological mechanisms of type 2 diabetes–induced vascular dysfunction, we induced a hyperglycemic state by competitively blocking insulin signaling through continuous infusion of S961, a high-affinity

peptide inhibitor of insulin receptor.<sup>18</sup> Moreover, pharmacology and physiological effects of the  $\beta_3$  ARs in the cardiovascular system are highly species-dependent, and since rabbits provide a relevant model for human  $\beta_3$  AR,<sup>19</sup> we characterized the metabolic and biochemical profile of S961-induced hyperglycemia in rabbits. We assessed endothelial function, measured  $\text{O}_2^{\bullet-}$  and NO levels in vessels and examined oxidative modification of eNOS and  $\text{Na}^+\text{-K}^+$  pump and relevant redox pathways that regulate these modifications. Subsequently, we assessed modulating effects of the  $\beta_3$  AR agonist CL316243 (CL) on these pathways/molecules and vascular function in this model.

## Materials and Methods

### S961-Induced Hyperglycemia, Animals, Cells, Treatments, and Hemodynamic and Metabolic Measurements

S961 was expressed in *Escherichia coli* as a fusion protein with an affinity tag and had the peptide sequence GSLDEFYDW-FERQLGGGSGSSLEEEWAQIQCEVWGRGCPSTY with a disulfide bridge connecting the 2 cysteine residues (a gift from Novo Nordisk, Denmark).<sup>18</sup> We infused S961 dissolved in normal saline for 7 days at a rate of 12  $\mu\text{g}/\text{kg}$  per hour via osmotic mini-pumps (Alzet, Palo Alto, CA) implanted subcutaneously in male New Zealand White rabbits, weighing 2.2 to 2.6 kg while they were under general anesthesia. The selective  $\beta_3$  AR agonist CL (Sigma-Aldrich, St. Louis, MO) was dissolved in normal saline and infused via mini-pumps at a rate of 40  $\mu\text{g}/\text{kg}$  per hour during the last 3 days of hyperglycemia. Since infusion of the vehicle alone (normal saline) in 5 rabbits did not change oxidative modification of the target proteins or endothelium-dependent vasorelaxation (either identical or almost-identical means within nearly equal SEM), we did not use sham infusions in controls. Durations of infusions of S961 and CL were limited by the amount of S961 we had available and the cost of CL needed in a relatively large animal such as rabbit. Blood samples for biochemical and metabolic analysis were obtained from the central ear artery of the anesthetized rabbits before and after each treatment. Blood glucose was measured in a drop of blood from the marginal ear vein using a glucometer and strips (Optium Xceed, Abbott Diabetes Care Ltd, Australia). Heart rate and blood pressure were measured via a catheter in the ear artery after anesthesia by subcutaneous injection of ketamine hydrochloride (50 mg/kg) and xylazine hydrochloride (50 mg/kg) prior to euthanasia by intravenous bolus injection of ketamine. The rabbit thoracic aorta was harvested and cleared of adhering tissue in Krebs buffer. The total number of rabbits used for this study was 50 (diabetogenesis with alloxan in vivo, n=9, control rabbits for in vitro assessment of diabetogenic agents n=6, sham infusions with normal saline n=5, control

rabbits for vasomotor studies and molecular experiments  $n=10$ , rabbits with hyperglycemia induced by S961 infusion including dose titration experiments  $n=20$ ). Pooled, multiple-donor human umbilical vein endothelial cells (Lonza, Basel, Switzerland) were used for in vitro experiments. Surplus segments of human internal mammary or radial artery were obtained from patients undergoing coronary artery bypass graft operation at our institution ( $n=4$  samples from diabetic patients and  $n=4$  from nondiabetic patients). Myocardial tissue was obtained from a patient undergoing cardiac biopsy at another institution. The study protocols were in accordance with institutional guidelines and were approved by the appropriate research ethics committees at our institution. Informed written consent was obtained from patients.

### Immunodetection of Glutathionylated Protein and Protein Co-Immunoprecipitation

To detect glutathionylation of eNOS and  $\beta_1$  Na<sup>+</sup>-K<sup>+</sup> pump subunit in co-immunoprecipitation experiments, an antibody against glutathionylated protein (anti-glutathione antibody) was used to detect glutathionylation.<sup>10</sup> Aorta was homogenized in ice-cold lysis buffer containing 150 mmol/L NaCl, 50 mmol/L Tris-HCl (pH 8.0), 1% Triton X-100, 2 mmol/L EDTA, and protease inhibitor (Complete EGTA-free, Roche Diagnostics), followed by centrifugation at 16 000g for 20 minutes. The supernatant (0.5–1 mg protein) was incubated with the appropriate antibody at a ratio of 1  $\mu$ g of  $\beta_1$  Na<sup>+</sup>-K<sup>+</sup> subunit antibody:1 mg protein and 2.5  $\mu$ g anti-eNOS antibody:1 mg protein at 4°C for 1 hour and then with protein A/G-Plus agarose beads. The proteins bound to the collected beads were eluted in Laemmli buffer, subjected to SDS-PAGE, and probed with anti-glutathione antibody. This protocol was also used to detect co-immunoprecipitation of eNOS/glutaredoxin-1 (Grx1),  $\beta_1$  subunit/Grx1, and p47<sup>phox</sup>/eNOS. To detect glutathionylation of  $\beta_1$  Na<sup>+</sup>-K<sup>+</sup> subunit in cardiac myocytes, freshly isolated myocytes were loaded with biotinylated glutathione ester (500  $\mu$ mol/L) for 1 hour at room temperature. The biotin-tag was used to precipitate glutathionylated proteins as previously described.<sup>10</sup> Western blot chemiluminescence was read by a LAS-4000 image reader and quantified by densitometry using Multi Gauge 3.1 software (Fujifilm Life Science, Tokyo, Japan). Exposure times were adjusted to ensure that the variation in signal intensity was in the linear dynamic range.

### Electron Paramagnetic Resonance Spin-Trapping Measurement of NO

To synthesize the colloid spin trap, sodium diethyldithiocarbamate (sodium DETC, 4.5 mg) and FeSO<sub>4</sub> 7H<sub>2</sub>O (2.8 mg) were dissolved separately in 10 mL of deoxygenated Krebs bubbled

with a nitrogen purge and mixed rapidly, resulting in a final concentration of Fe(DETC)<sub>2</sub> of 0.5 mmol/L. The spin trap was used immediately. After harvesting the aorta from rabbits and separating the loose adhering tissue, the aorta was opened longitudinally and cut into 10×10 mm segments. The segments were placed in a 6-well plate containing 500  $\mu$ L Krebs, with 500  $\mu$ L of Fe(DETC)<sub>2</sub> added (final concentration of 0.25 mmol/L), and incubated at 37°C for 30 minutes. The tissue samples were placed in electron paramagnetic resonance tubes, snap-frozen, and stored at –80°C until analysis. Spectra were recorded at 77 K with a Bruker EMX X-band spectrometer using the following parameters: microwave power 2.5 mW; microwave frequency 9.4 GHz; modulation amplitude 0.2 mT; modulation frequency 100 kHz; conversion time 81.9 ms, time constant 163.8 ms, scan time 83.9 s with 12 scans averaged. The amplitude of NO signal was determined as the perpendicular height between the top of the first low-field signal and the valley of the third high-field signal.<sup>20</sup>

### High-Performance Liquid Chromatography Analysis of Dihydroethidium (DHE) Oxidation Products

The stock solution of DHE was prepared by dissolving DHE in deoxygenated dimethyl sulfoxide under argon in the dark with the concentration checked by UV-VIS. Immediately after harvesting from rabbits, five 2-mm segments of aorta were incubated in Krebs buffer containing the metal chelator diethylenetriaminepentaacetic acid (DTPA, 100  $\mu$ mol/L) to minimize artificial oxidation, and DHE (50  $\mu$ mol/L) in 1.5 mL Eppendorf tubes (37°C, 30 minutes, in the dark). The tissue was washed of the DHE with Krebs/DTPA 3 times and homogenized in 300  $\mu$ L of cold methanol by centrifugation at 12 000g for 10 minutes at 4°C in the dark. Fifty microliters of homogenate was taken to determine protein concentration. Equal amounts of the homogenate were then added to equal amount of 0.2 mol/L of HClO<sub>4</sub> in methanol, vortexed, and placed on ice for 1 hour in the dark to allow precipitation of protein. After centrifugation at 20 000g at 4°C for 30 minutes, the supernatant was stored at –80°C until analysis. High-performance liquid chromatography equipped with a fluorescence and a CoulArray electrochemical detector was used to separate the O<sub>2</sub><sup>•-</sup>-dependent 2-hydroxy-ethidium (2-OH-E<sup>+</sup>) product from the nonspecific product ethidium (E<sup>+</sup>) following DHE oxidation in rabbit aorta.<sup>21</sup> Samples (50  $\mu$ L) were separated by high-performance liquid chromatography (Shimadzu) after injection onto a Synergi Polar RP C18 column (250×4.6 mm, 4  $\mu$ mol/L, 80 Å, Phenomenex) equilibrated at 30°C with 60% mobile phase A (10% CH<sub>3</sub>CN in potassium phosphate buffer, 50 mmol/L, pH 2.6) and 40% mobile phase B (60% CH<sub>3</sub>CN in potassium phosphate buffer, 50 mmol/L, pH 2.6). Separation of products was performed

by a linear increase to 100% mobile phase B over 30 minutes at a flow rate of 0.5 mL min<sup>-1</sup>. Products were quantified by fluorescence (DHE and 2-OH-E<sup>+</sup>:  $\lambda_{EX}$  358 nm,  $\lambda_{EM}$  440 nm; E<sup>+</sup>  $\lambda_{EX}$  490 nm,  $\lambda_{EM}$  565 nm) and electrochemical oxidation using a CoulArray detector (Environmental Sciences Associates; electrodes at 0, 200, 280, 365, 400, 450, 500, and 600 mV). The quantified 2-OH-E<sup>+</sup> levels were normalized to protein concentration.

## Aortic Preparation and Functional Measurements

Aortic rings measuring 5 mm in length were mounted on 2 stainless steel hooks immersed in 25 mL organ bath chambers filled with Krebs buffer containing (in mmol/L) NaCl 118, KCl 4.6, NaHCO<sub>3</sub> 27.2, MgSO<sub>4</sub> 1.2, CaCl<sub>2</sub> 2.5, KH<sub>2</sub>PO<sub>4</sub> 1.2, and glucose 11.1 (pH 7.4). The isometric contractions were measured in organ chambers at 37°C by using a force transducer (Radnoti) and recording with Powerlab software (AD Instruments, United States). Vascular rings were allowed to equilibrate for 0.5 hours and tension was gradually increased to 2 g. Vessels were then contracted with the addition of 80 mmol/L KCl to determine integrity of the rings. After maximum contraction was achieved, the aortic rings were washed with Krebs buffer and re-equilibrated. Rings were then precontracted with phenylephrine (100 nmol/L). Once a plateau was achieved, increasing concentrations of acetylcholine were added. The endothelium-dependent relaxation was expressed as the percentage of relaxation to phenylephrine-induced contraction. In separate experiments, Krebs buffer was replaced with Krebs buffer that was nominally K<sup>+</sup>-free. After 20 minutes in K<sup>+</sup>-free Krebs buffer, rings were precontracted with phenylephrine (100 nmol/L). Once a plateau was achieved, increasing concentrations of K<sup>+</sup> were administered as previously described.<sup>22,23</sup> As the Na<sup>+</sup>-K<sup>+</sup> pump is inhibited in the absence of extracellular K<sup>+</sup> and reactivated by its reintroduction at low concentrations, K<sup>+</sup>-induced relaxation has been characterized as an index of Na<sup>+</sup>-K<sup>+</sup> pump activity in arteries, which is dependent on external K<sup>+</sup> and intracellular Na<sup>+</sup> and Mg<sup>2+</sup> and inhibited by the pump inhibitor ouabain.<sup>22</sup>

## Materials

Sodium diethyldithiocarbamate, FeSO<sub>4</sub> 7H<sub>2</sub>O, diethylenetriaminepentaacetic acid, and glutathione ethyl ester were purchased from Sigma-Aldrich. N-Hydroxysulfosuccinimidobiotin was obtained from Merck, dithiothreitol from Promega, streptavidin–Sepharose from GE Healthcare Bio-Sciences, and Protein A/G-Plus agarose from Santa Cruz Biotechnology. Osmotic mini-pumps were purchased from Alzet and CL from Sigma-Aldrich. Dihydroethidium and *N*-(Biotinoyl)-*N'*-(iodoacetyl) ethylenediamine were obtained from Invitrogen. Mono-

clonal antibodies were purchased from the following vendors:  $\beta_1$  subunit of Na<sup>+</sup>-K<sup>+</sup> ATPase from Upstate Biotechnology; anti-glutathione from Virogen, eNOS antibody from Sigma-Aldrich, and p47<sup>phox</sup>, phosphorylated eNOS116, phosphorylated eNOS117, neuronal NOS (nNOS), and  $\alpha$  tubulin from Santa Cruz Biotechnology. All chemicals used in Krebs solutions were analytical grade and were obtained from BDH.

## Statistical Analysis

Results are presented as mean $\pm$ SEM and median with 25% to 75% interquartile range where necessary. Kolmogorov–Smirnov test was performed to check for normality. For comparison between 2 groups either a non-paired Student *t* test or a Mann–Whitney test were used where appropriate. Paired *t* test was used for analysis of changes in blood biochemistry and body weight before and after the induction of hyperglycemia or treatment with CL (Table). For multiple comparisons, 1-way ANOVA was used with Tukey's post-hoc analysis. For vasorelaxation data, concentrations of acetylcholine and vasorelaxation responses in rabbits from different experimental groups were included in 2-way repeated-measures ANOVA with Tukey or Sidak's post-hoc tests used for multiple comparisons. *P* value <0.05 was considered statistically significant.

## Results

### Choice of Hyperglycemia Model to Avoid Redox Effects of Diabetogenic Agents

Since we aimed to examine the effects of hyperglycemia on oxidative modification of proteins, we first determined whether alloxan and STZ, agents commonly used to establish type 1 diabetes, would have direct redox effects independently of diabetes per se. We tested this by examining glutathionylation of the highly abundant, ubiquitous membrane protein Na<sup>+</sup>-K<sup>+</sup> pump, which mediates inhibition of the pump function in cardiac myocytes<sup>24</sup> and vascular smooth muscle cells.<sup>23</sup> Alloxan, at high concentrations in vitro (1 mmol/L, 37°C, 30 minutes), reflecting the pancreatotoxic diabetogenic doses used in vivo, increased glutathionylation of the  $\beta_1$  Na<sup>+</sup>-K<sup>+</sup> pump subunit (Figure 1A). Moreover, glutathionylation of the  $\beta_1$  pump subunit was also increased in rabbits that received a typically diabetogenic dose of alloxan (100 mg/kg) in vivo but did not develop diabetes due to insufficient necrosis of pancreatic  $\beta$  cells (Figure 1B). Higher glutathionylation levels were detected 7 days after alloxan injection and were similar to levels in rabbits that did develop diabetes (Figure 1B), thus showing that alloxan can alter glutathionylation independent of diabetogenesis in vivo. In contrast, exposure of isolated rabbit cardiac myocytes to

**Table.** Metabolic, Biochemical and Hemodynamic Effects of the Insulin Receptor Antagonist S961 and the β3 AR Agonist CL

	Baseline	Hyperglycemia		
Weight, kg	2.4±0.2	2.7±0.2*		
Na <sup>+</sup> , mmol/L	143.5±7.4	140.2±3.8		
K <sup>+</sup> , mmol/L	4.4±0.2	3.9±0.4		
Urea, mmol/L	6.5±2.1	5.7±2.8		
Creatinine, mmol/L	67.8±11.3	50.3±11.9		
Triglyceride, mmol/L	1.3±1.0	2.2±1.1		
Cholesterol, mmol/L	1.5±0.4	1.0±0.5		
Insulin, mIU/L	<3	121.2±54*		
C-peptide, pmol/L	<33	<33		
			Pre CL	Post CL
Blood glucose, mmol/L			15.9±0.7	17±0.6
Plasma insulin, mIU/L			104.9±1.1	132.5±17.5
	Control	CL	HG	HG+CL
Heart rate	204±6	212±5	205±5	200±3
Systolic blood pressure	93±2	78±5*	90±2	79±2*
Diastolic blood pressure	82±2	66±5*	76±2	63±2*
Mean arterial pressure	86±2	70±3*	81±2	68±2*

Body weight, electrolytes, renal function, lipid profile, insulin, and C-peptide levels in rabbits at baseline and after 7 days of infusion with S961 at 12 μg/kg per hour. n=8. Heart rate, systolic, diastolic, and mean arterial pressure in rabbits with S961 hyperglycemia (HG) and after the infusion of the selective β3 AR agonist CL316243 (CL, 40 μg/kg per hour, 3 days). n=10. Blood glucose and insulin levels in S961 hyperglycemic rabbits pre- and postinfusion of CL (40 μg/kg per hour, 3 days). n=5. β3 AR indicates β3 adrenergic receptors; IU, international units.

\*Statistical significance.

STZ in vitro (37°C, 30 minutes) decreased glutathionylation of β<sub>1</sub> Na<sup>+</sup>-K<sup>+</sup> pump subunit in a concentration-dependent manner (Figure 1C). In contrast, S961, the peptide antagonist of the insulin receptor, had no effects on β<sub>1</sub> pump subunit glutathionylation in vitro (Figure 1D).

### Metabolic and Biochemical Parameters and Vascular Phenotype of S961-Induced Hyperglycemia

The details of how we determined the appropriate dose of S961 to establish stable, persistent hyperglycemia is described by us elsewhere.<sup>25</sup> Briefly, after checking for transient hyperglycemia induced by a bolus injection of S961 in rabbits, we examined the effects of continuous subcutaneous infusion at different rates, and found that mean blood glucose values increased with an increase in the rate of S961 infusion.<sup>25</sup> On the basis of our dose titration experiments, we selected an infusion rate of 12 μg/kg per hour for the study. Continuous S961 infusion at this rate induced a relatively rapid rise in blood glucose levels in rabbits that remained stably high during the 7 days of infusion (Figure 2A). Since infusion of vehicle (normal saline) alone in 5 rabbits had no effect oxidative modification of the target proteins (data not

shown), we did not use sham infusions in controls. Mean blood glucose levels in rabbits infused for 7 days with this rate compared to levels in controls are shown in Figure 2B. The S961-induced increase in blood glucose levels was associated with an increase in plasma insulin levels (Table) consistent with a counter-regulatory response to the competitive insulin receptor blockade shown in in vitro studies.<sup>18</sup> C-peptide levels were not within the detection limits of the assay (Table). The rabbits gained weight normally during the study (Table). S961 infusion had no effect on serum Na<sup>+</sup> or K<sup>+</sup>, renal function, and cholesterol or triglyceride levels (Table). To examine the impact of S961 model on vascular physiology, we measured endothelium-dependent relaxation in aortic rings precontracted with phenylephrine in organ chambers. S961 hyperglycemia reduced acetylcholine-induced relaxation (Figure 2C). In contrast, sodium nitroprusside-induced relaxation was unchanged (Figure 2D).

### Effects of β3 AR Agonism on NO- and O<sub>2</sub><sup>•-</sup> Levels, eNOS Uncoupling, and Endothelial Function in S961 Model

We co-administered the β3 AR agonist CL by continuous infusion in hyperglycemic rabbits for the last 3 days of the

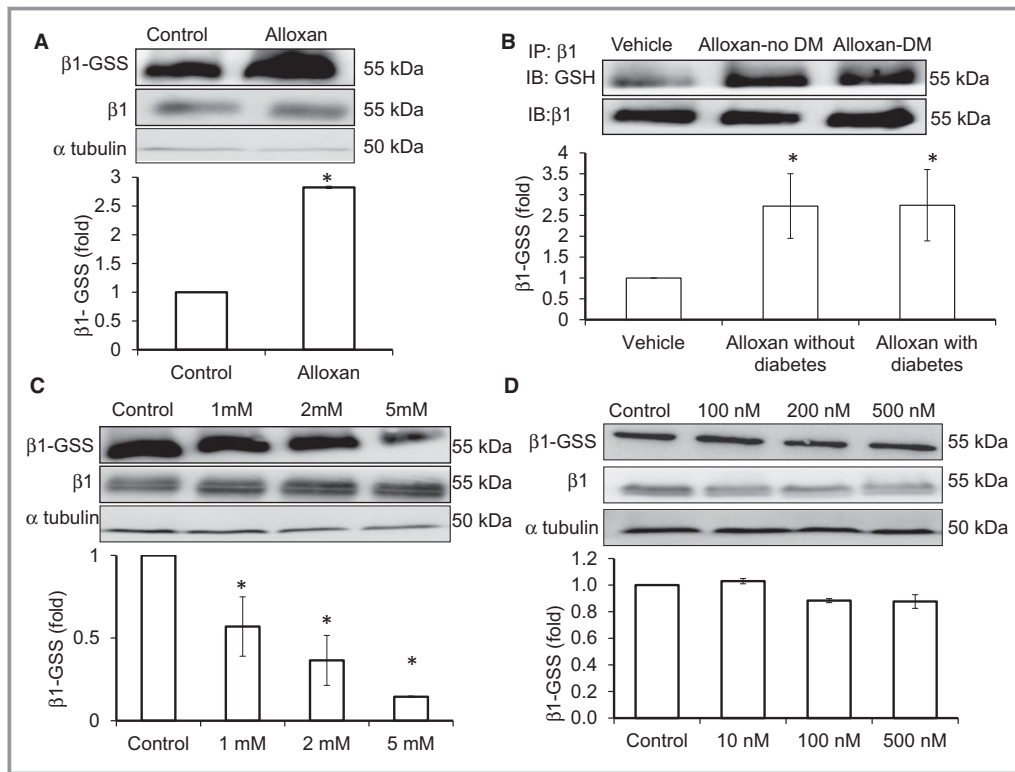


**Figure 1.** Effects of diabetogenic agents on redox modification of the Na<sup>+</sup>-K<sup>+</sup> pump. A, Effect of alloxan on β<sub>1</sub> Na<sup>+</sup>-K<sup>+</sup> pump glutathionylation (β<sub>1</sub>-GSS) in isolated rabbit cardiac myocytes loaded with biotinylated glutathione (BiOGEE technique) prior to alloxan exposure (n=5). B, β<sub>1</sub>-GSS in rabbits receiving a bolus injection of alloxan (100 mg/kg) with and without developing diabetes, as detected by immunoblots (IB) with anti-glutathione and anti-β<sub>1</sub> subunit antibodies in the β<sub>1</sub> subunit immunoprecipitate (IP). C, Effect of STZ on β<sub>1</sub>-GSS examined by BiOGEE technique (n=5). D, Effect of S961 on β<sub>1</sub>-GSS (n=6). α tubulin was used as loading control. Statistical significance is indicated by \*. STZ indicates streptozocin.

study. Treatment with CL had no effect on plasma glucose or insulin levels (Table). CL also had no effect on heart rate but it reduced blood pressure (Table). S961-induced hyperglycemia impaired endothelial function as measured by acetylcholine-induced relaxation in aortic rings of hyperglycemic rabbits, which was restored by in vivo CL treatment (Figure 3A). There was a marked increase in O<sub>2</sub><sup>•-</sup> levels in aorta of hyperglycemic rabbits as measured by 2-OH-E<sup>+</sup> levels, the specific product of DHE oxidation by O<sub>2</sub><sup>•-</sup> (Figure 3B). Treatment with CL reduced O<sub>2</sub><sup>•-</sup> levels in aorta of hyperglycemic rabbits (Figure 3B). While NO levels, measured by electron paramagnetic resonance analysis of NO-Fe(DETC)<sub>2</sub> complexes, were decreased in aorta of hyperglycemic rabbits, they were restored to almost normal levels by treatment with CL (Figure 3C).

Since hyperglycemia was associated with increased O<sub>2</sub><sup>•-</sup> and decreased NO levels, we next examined whether hyperglycemia had induced eNOS uncoupling. Indeed, consistent with the pattern of changes in the free radicals, we found an increase in eNOS glutathionylation in aorta of hyperglycemic rabbits (Figure 3D). In vivo infusion of CL abolished the increase in hyperglycemia-induced eNOS

glutathionylation (Figure 3D). Taken together, these data show that CL enhances NO bioavailability, decreases oxidative stress, recouples eNOS, and improves endothelial function in S961-induced hyperglycemia.

### Effect of β<sub>3</sub> AR Agonism on Redox Regulation of the Vascular Na<sup>+</sup>-K<sup>+</sup> Pump in S961-Induced Hyperglycemia

Since the Na<sup>+</sup>-K<sup>+</sup> pump plays a major role in regulation of many essential cellular processes in the vasculature including regulation of vascular tone, we next examined the effects of CL on the function of the pump, previously reported by our group to be regulated by redox-dependent mechanisms in the vasculature.<sup>23</sup> Hyperglycemia decreased K<sup>+</sup>-induced relaxation, which is dependent on Na<sup>+</sup>-K<sup>+</sup> pump reactivation upon a switch from nominally K<sup>+</sup>-free to K<sup>+</sup>-containing solutions in the tissue bath<sup>22</sup> (Figure 4A). CL enhanced K<sup>+</sup>-induced relaxation in aortic rings of hyperglycemic rabbits (Figure 4A). Consistent with this functional effect, CL abolished hyperglycemia-induced increase in β<sub>1</sub> subunit glutathionylation (Figure 4B).

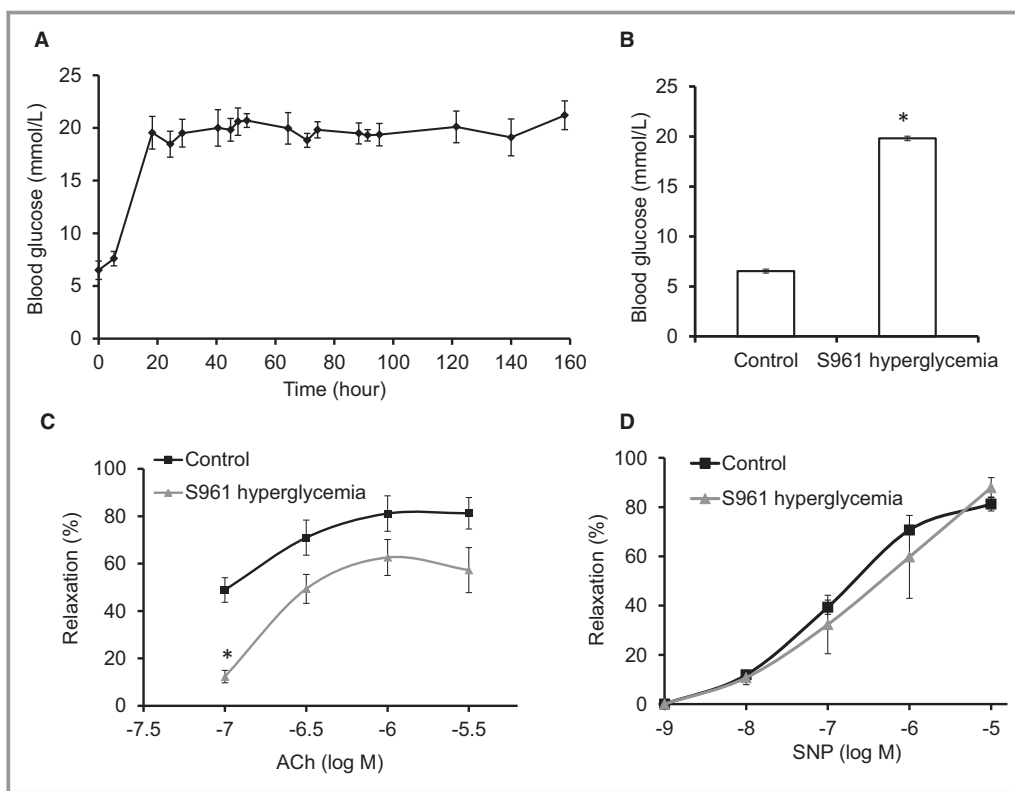


**Figure 2.** Blood glucose levels and vascular function in S961-induced hyperglycemia. A, Blood glucose levels of rabbits infused subcutaneously via osmotic mini-pump with S961 (12 μg/kg per hour). (n=5). B, Mean blood glucose levels of control rabbits and rabbits with S961-induced hyperglycemia over 7 days (n=10). C, Endothelium-dependent vasorelaxation in aortic rings of control and hyperglycemic rabbits (n=6 control and 5 hyperglycemic rabbits, with 2–3 or 3–5 rings studied per rabbit in each group, respectively). These baseline data are re-presented in Figure 3A. *P*=0.01 on 2-way repeated-measures ANOVA. D, SNP-induced vasorelaxation in control and diabetic rabbits (n=6 rabbits and 2–3 rings per rabbit). *P*=0.69 on 2-way repeated-measures ANOVA. Relaxations are plotted as the percentage decrease in PE-induced contraction against the concentration of ACh or SNP on a logarithmic scale. PE-induced contractions were not different across different groups. Statistical significance is indicated by \*. ACh indicates acetylcholine; PE, phenylephrine; SNP, sodium nitroprusside.

### Effect of β<sub>3</sub> AR Agonism on Sources of ROS and Antioxidant Pathways in S961-Induced Hyperglycemia

Because O<sub>2</sub><sup>•-</sup> levels were significantly higher in vessels of hyperglycemic rabbits, and since NADPH oxidase is a major source of vascular O<sub>2</sub><sup>•-</sup> in diabetes, we examined whether activation of the oxidase contributed to the redox stress in hyperglycemia. Aortic rings from control and hyperglycemic rabbits were incubated with the membrane-permeable peptide gp91ds-tat ex vivo. The peptide had no effect on acetylcholine-induced relaxation in control rings (Figure 5A), but it improved relaxation in rings from hyperglycemic rabbits (Figure 5B), suggesting that increased constitutive NADPH oxidase activity contributed to the hyperglycemia-induced endothelial dysfunction. Accordingly, gp91ds-tat had no effect on eNOS glutathionylation in control rabbits (Figure 5C), but it decreased eNOS glutathionylation in aorta of hyperglycemic rabbits (Figure 5D).

Activation of NADPH oxidase depends on translocation of its cytosolic p47<sup>phox</sup> subunit to the membrane, a translocation that is blocked by the cell-permeable peptide gp91ds-tat. We examined co-immunoprecipitation of p47<sup>phox</sup> subunit with eNOS as an index of p47<sup>phox</sup> translocation to the membrane. p47<sup>phox</sup>/eNOS co-immunoprecipitation was increased in hyperglycemic rabbits, with CL treatment significantly reducing it (Figure 5E), thus pointing to a probable effect of CL in decreasing hyperglycemia-induced activation of the oxidase.

Glutathionylation is a reversible reaction, with de-glutathionylation catalyzed by Grx1. Since activation of Grx1 is believed to occur via translocation to its targets,<sup>26</sup> we examined association of Grx1 with eNOS and β<sub>1</sub> Na<sup>+</sup>-K<sup>+</sup> pump subunit by co-immunoprecipitation as a surrogate for its activation. While co-immunoprecipitation of both eNOS/Grx1 and β<sub>1</sub> pump subunit/Grx1 was markedly decreased in hyperglycemia, CL treatment significantly increased these associations without changing Grx1 abundance (Figure 5F),

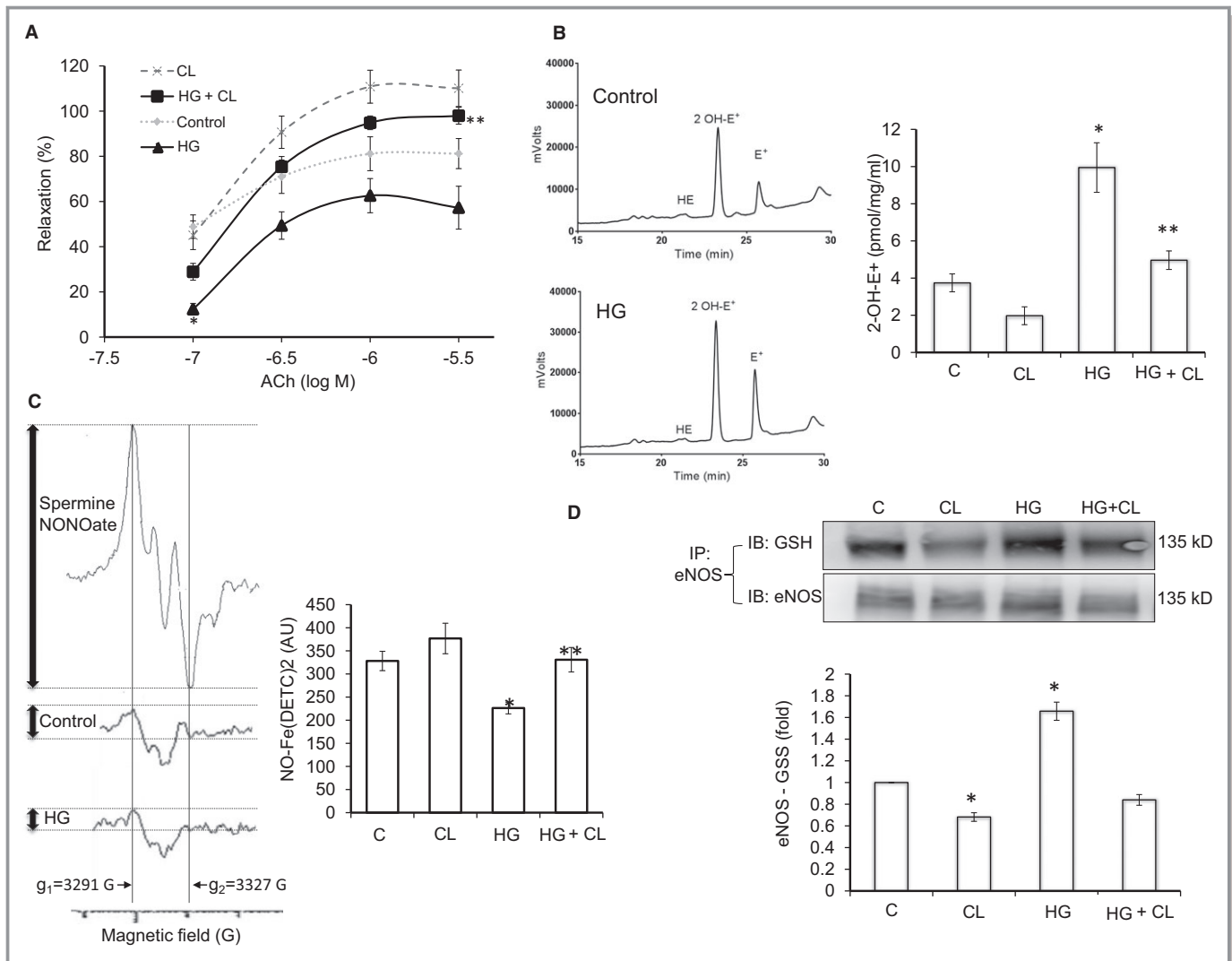


**Figure 3.** Effect of β<sub>3</sub> AR agonism on endothelial function, NO- and O<sub>2</sub>•<sup>-</sup> levels, and redox modification of eNOS in S961-induced hyperglycemia. A, Effect of CL316243 (CL) on ACh-induced relaxation in aorta of control and hyperglycemic rabbits. Number of rabbits per each group: 6 controls (2–3 rings/rabbit), 5 hyperglycemics (3–5 rings/rabbit), 5 CL-treated controls (4–6 rings/rabbit), and 6 CL-treated hyperglycemics (HG) (3–6 rings/rabbit). P=0.01 (control vs HG) and 0.005 (HG vs HG+CL) on 2-way repeated-measures ANOVA. B, O<sub>2</sub>•<sup>-</sup> levels in rabbit aorta by HPLC analysis of the specific- (2-OH-E<sup>+</sup>) and nonspecific product (E<sup>+</sup>) of DHE oxidation. Representative chromatograms from a control and a hyperglycemic rabbit are shown. [2-OH-E<sup>+</sup>]=mean values over protein concentration (pmol/mg per mL). n=5 control, 5 CL-treated, 6 hyperglycemic- and 5 CL-treated hyperglycemic rabbits. C, NO measurement by electron paramagnetic resonance of Fe(DETC)<sub>2</sub> in rabbit aorta. The amplitude of NO-Fe(DETC)<sub>2</sub> signal was determined as the height between the top of the first low field signal (g<sub>1</sub>=3291 G) and the valley of the third high field signal (g<sub>2</sub>=3327 G) (up–down double arrows on the left). The trace from the standard spermine NONOate in dimethyl sulfoxide solution is shown. n=7 control-, 4 CL-treated-, 5 hyperglycemic-, and 5 CL-treated hyperglycemic rabbits. D, Glutathione and eNOS immunoblot (IB) of eNOS immunoprecipitate (IP) from rabbit aorta. n=5. \*P<0.05 vs control and \*\*P<0.05 vs hyperglycemia. eNOS indicates endothelial nitric oxide synthase.

thus suggesting that CL might have enhanced de-glutathionylation by Grx1.

### Effect of β<sub>3</sub> AR Agonism on eNOS Glutathionylation in Human Diabetes

To assess the relevance of our findings in the S961 model of hyperglycemia to human diabetes, we examined the changes in eNOS glutathionylation in vessels harvested from diabetic

patients and their matched controls (both groups had hypertension, dyslipidemia, and ischemic heart disease with no differences in age [70±3 versus 69±4 years]). Similar to the experimental model, there was an increase in eNOS-GSS in vessels of diabetic patients (Figure 6A). CL stimulated NO release in human endothelial cells (Figure 6B) and it decreased the levels of eNOS-GSS in the vessels of diabetic patients (Figure 6C). In contrast to signaling in cardiac myocytes, β<sub>3</sub> AR stimulation in human vessels was not

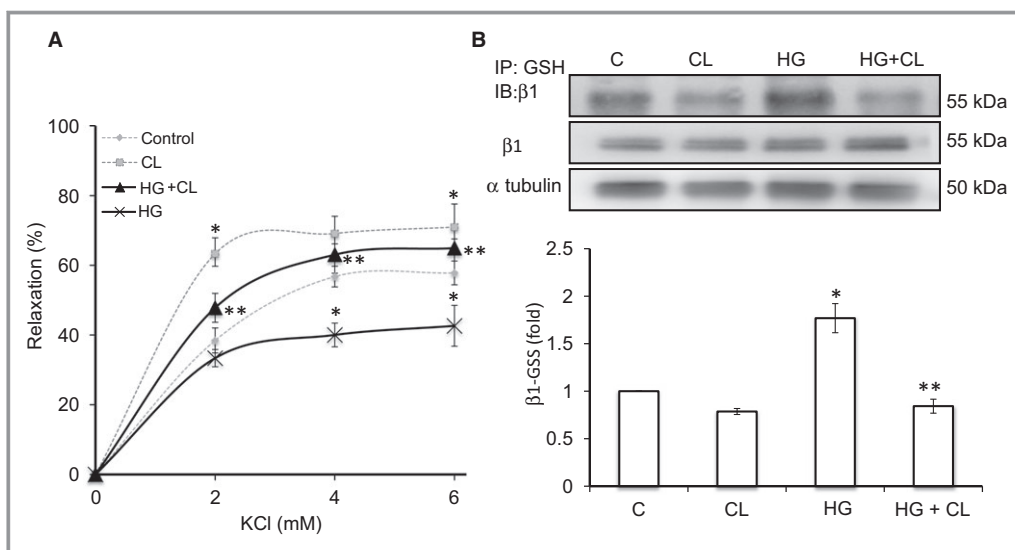


**Figure 4.** β<sub>3</sub> AR stimulation and redox regulation of the vascular Na<sup>+</sup>-K<sup>+</sup> pump in S961-induced hyperglycemia. A, Effect of CL on K<sup>+</sup>-induced relaxation in aortic rings of control- and hyperglycemic rabbits. n=7 control- (2–4 rings/rabbit), 5 hyperglycemic- (2 rings/rabbit), 4 CL-treated- (4–6 rings/rabbit), 6 CL-treated hyperglycemic- (4–6 rings/rabbit) rabbits. P=0.01 (HG vs control), 0.02 (CL vs control) and 0.001 (HG vs HG+CL) on 2-way repeated-measures ANOVA. B, Glutathionylated β<sub>1</sub> subunit detected by glutathione antibody technique. β<sub>1</sub> Na<sup>+</sup>-K<sup>+</sup> pump subunit IB of the glutathione IP is shown on top row. IB of β<sub>1</sub> subunit and α tubulin from raw homogenates of rabbit aorta are also shown. n=5. \*P<0.05 vs control and \*\*P<0.05 vs hyperglycemia. HG indicates hyperglycemia; IB, immunoblot; IP, immunoprecipitate.

mediated by differential phosphorylation of eNOS<sup>27,28</sup> (Figure 7A) nor through nNOS<sup>28</sup> as we did not detect a signal for nNOS expression in human endothelial cells or vessels of diabetic and nondiabetic patients, regardless of exposure to CL (Figure 7B). This might be due to very low constitutive expression of nNOS in endothelial cells.<sup>29</sup> Taken together, these human data suggest the presence and support the potential significance of the redox pathways that we have examined in detail in the S961 model.

## Discussion

We have established a model of persistent hyperglycemia by competitive antagonism of insulin receptor by S961 and describe the pathophysiological vascular phenotype of the model. We set out to determine the redox effects of β<sub>3</sub> AR stimulation in experimental hyperglycemia and it was important to first examine whether diabetes-inducing agents have confounding effects on the target proteins of interest. The most commonly used diabetogenic agent STZ, a glucosamine-nitrosourea taken up by pancreatic β cells causing their necrosis,<sup>30</sup> decreased the oxidative modification of β<sub>1</sub> Na<sup>+</sup>-K<sup>+</sup> pump subunit in vitro. With short in vitro exposure time, this is likely due to the property of STZ to release NO,<sup>31</sup> shown to reduce β<sub>1</sub> subunit glutathionylation.<sup>11</sup> When administered at high toxic doses in vivo, STZ increases cellular ROS levels and causes undesirable extrapancreatic genotoxic effects that

further complicate differentiation of STZ direct molecular effects from effects of diabetes that it induces.<sup>30</sup> Alloxan, the second most commonly used diabetogenic agent, increased β<sub>1</sub> pump subunit glutathionylation both in vitro and in vivo independently of diabetogenesis. These effects are consistent with ROS generation and thiol oxidizing properties of alloxan.<sup>32</sup> In contrast to STZ and alloxan, S961 peptide had no effect on oxidative modification of β<sub>1</sub> pump subunit in vitro, suggesting that it did not have direct redox effects on the Na<sup>+</sup>-K<sup>+</sup> pump.

Effects of single injections of S961 on blood glucose over a period of hours have been previously reported.<sup>18</sup> Here we show that blood glucose rises rapidly and remains stable when S961 is administered at a constant rate, contrasting the early instability that often includes life-threatening hypoglycemia after injection of STZ or alloxan. It is an advantage of this new model that blood glucose levels are readily titrated to a target range with a change in infusion rate.<sup>25</sup> The model also allows cessation of infusion at any time and hence studying the reversibility of the effects caused by the hyperglycemic state. We detected no effect on metabolic variables except serum glucose for the duration of S961 infusion and, importantly, no effects on nutritional status or ketoacidosis, a complication often seen in alloxan- and STZ-induced diabetes. Ketoacidosis increases ROS generation independently of hyperglycemia.<sup>30</sup> Of mechanistic importance, S961 provides a model of hyperglycemia and insulin signaling

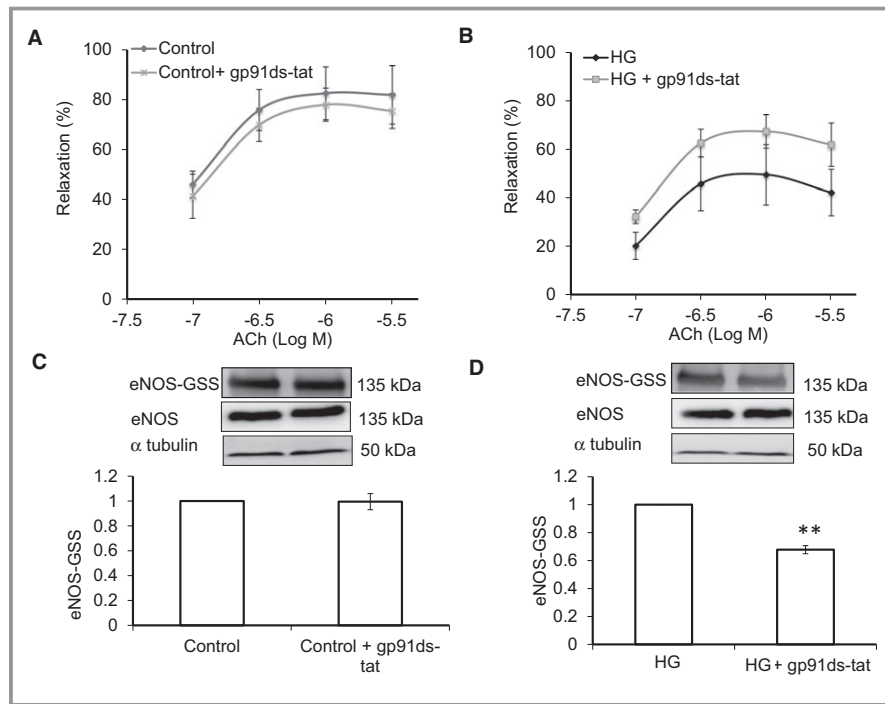


**Figure 5.** Effect of β<sub>3</sub> AR agonism on sources of ROS and de-glutathionylation enzymatic system in hyperglycemia. A and B, ACh-induced relaxation in aortic rings from control and hyperglycemic rabbits with and without ex vivo incubation with gp91ds-tat (5 μmol/L, 37°C, 1 hour) prior to vasomotor studies. n=5 control and 5 hyperglycemic rabbits with 3 rings pre-incubated vs 3 rings not pre-incubated with gp91ds-tat (5 μmol/L, 37°C, 1 hour) in each rabbit. P=0.15 in controls and 0.01 in hyperglycemics on 2-way repeated-measures ANOVA. C and D, eNOS IB of glutathione IP from rabbit aorta with and without ex vivo exposure and α tubulin IB as loading control are shown. n=5. E, p47<sup>phox</sup> and eNOS IB of p47<sup>phox</sup> IP from rabbit aorta n=5. F, Glutaredoxine-1 (Grx1), β<sub>1</sub> Na<sup>+</sup>-K<sup>+</sup> pump subunit (β<sub>1</sub>), and eNOS IB of Grx1 IP from rabbit aorta. n=5. Grx1/Grx1 co-immunoprecipitation was unaltered between the groups. The panels show the mean of signal for the groups. \*P<0.05 vs control and \*\*P<0.05 vs hyperglycemia. β<sub>3</sub> AR indicates β<sub>3</sub> adrenergic receptors; ACh, acetylcholine; CL, CL316243; eNOS, endothelial nitric oxide synthase; GSS, glutathionylation; HG, hyperglycemia; IB, immunoblot; IP, immunoprecipitate; ROS, reactive oxygen species.

blockade, central features in pathobiology of vascular disease in diabetes<sup>16,17</sup> as opposed to the commonly used insulinopenic hyperglycemia models where insulin signaling is usually unaltered. In this study we infused S961 for 7 days. However, in principle, it should be possible to use the model for the study of hyperglycemia for longer durations.

In S961-induced hyperglycemia, we show that activation of β<sub>3</sub> ARs improves endothelial function through modulation of oxidative pathways that lead to recoupling of eNOS and re-establishment of NO/redox balance (summarized in Figure 8). Although these effects are shown in relatively short-term hyperglycemia, our recent report of protective effects of β<sub>3</sub> AR agonism in the heart in hyperglycemic state,<sup>25,33</sup> the close similarities of β<sub>3</sub> AR-induced redox effects with angiotensin-converting enzyme inhibitors,<sup>7</sup> and presence of the β<sub>3</sub> AR-mediated effects in vascular tissue of diabetic patients we

show here point to potential therapeutic benefit of β<sub>3</sub> AR agonists for cardiovascular protection in diabetes.

S961 infusion increased vascular levels of ROS, recapitulating a central feature in the pathophysiology of diabetes-induced vascular disease. The effects of gp91ds-tat to increase endothelium-dependent vasorelaxation and to reduce eNOS glutathionylation in aorta of hyperglycemic rabbits as opposed to no effects in controls suggest that NADPH oxidase is pathologically activated in the vasculature of hyperglycemic rabbits and that its activation is upstream to glutathionylation-mediated eNOS uncoupling and endothelial dysfunction. This is consistent with NADPH oxidase as the major source of ROS in other experimental models of diabetes<sup>34</sup> and vessels of diabetic humans.<sup>35</sup> Since gp91ds-tat prevents docking of the cytosolic p47<sup>phox</sup> subunit to the membranous gp91<sup>phox</sup>, the isoforms activated in S961

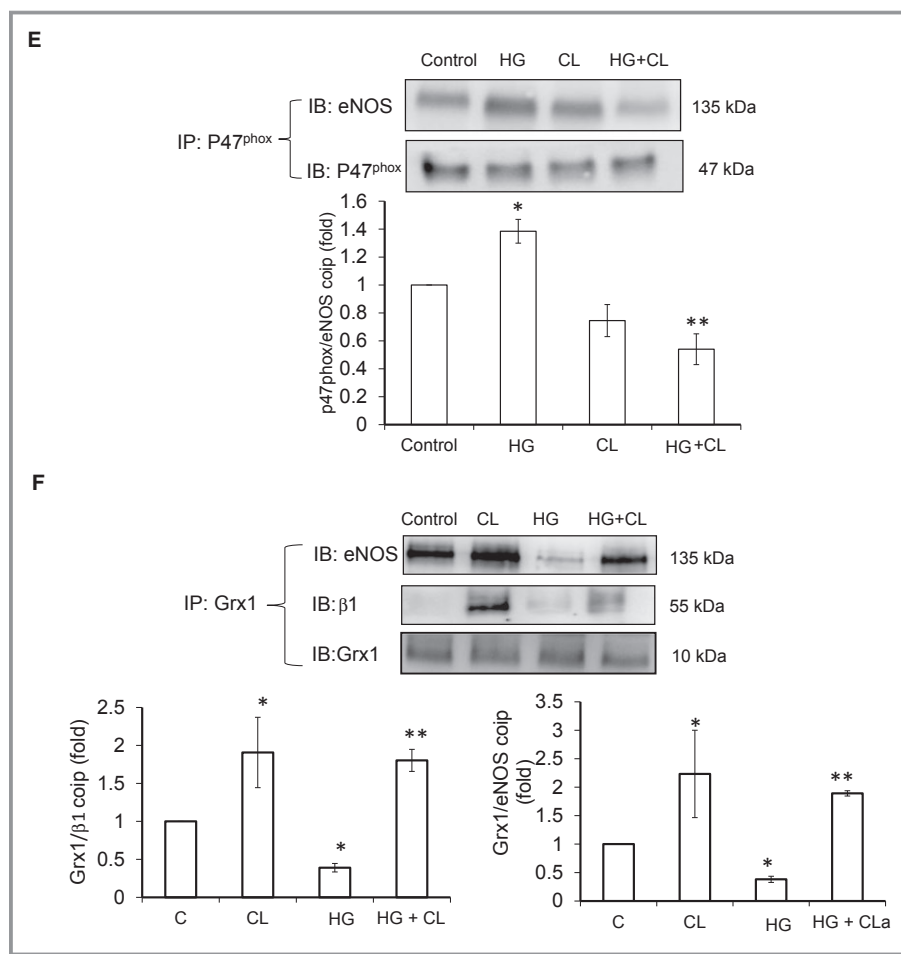
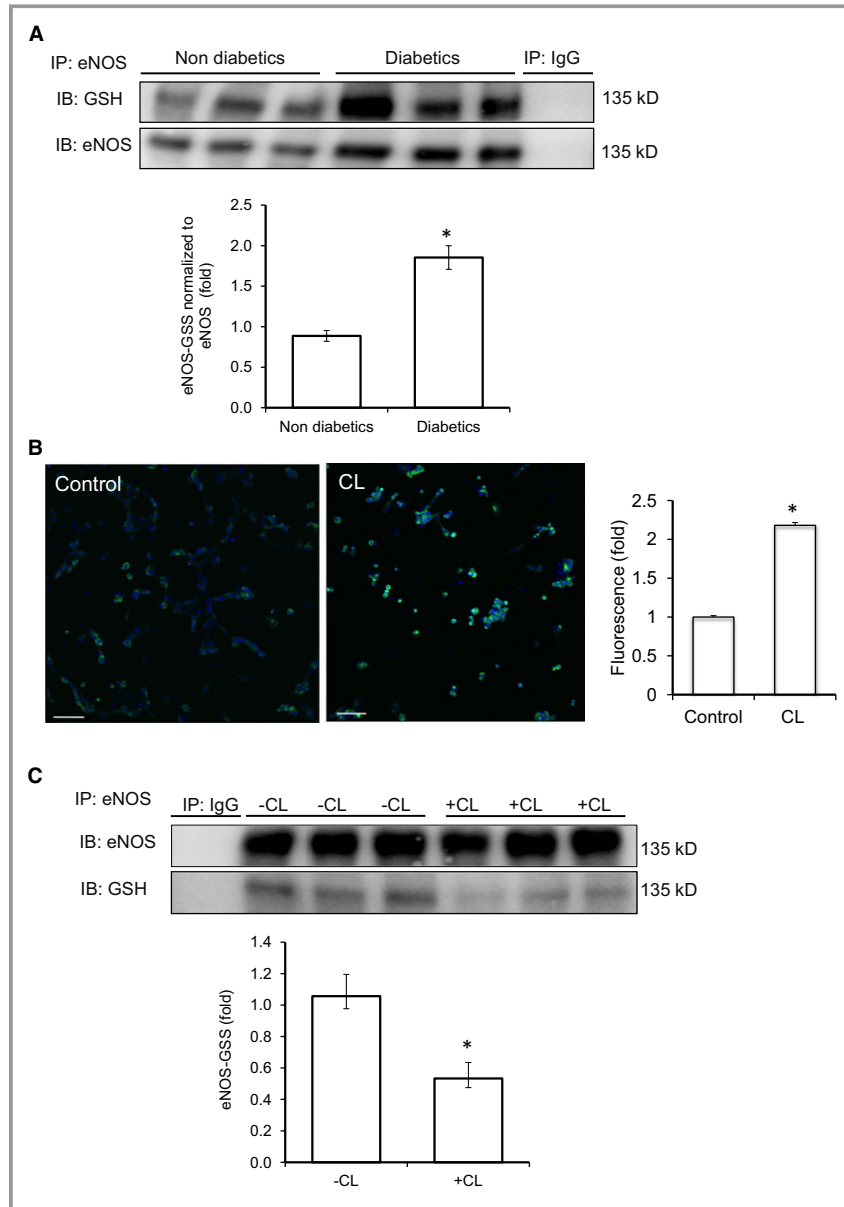


Figure 5. continued.

hyperglycemia are likely Nox1 or Nox2, which require p47<sup>phox</sup> translocation to membrane.<sup>2</sup> Consistent with this, we detected an increase in co-immunoprecipitation of p47<sup>phox</sup> with eNOS, a surrogate for association/translocation of the subunit to membrane, in aorta of hyperglycemic rabbits. Complex interactions between membrane and cytosolic sources of ROS such as mitochondria and xanthine oxidase in endothelial cells have been previously shown.<sup>36</sup> Although we implicate NADPH oxidase-mediated eNOS uncoupling as an upstream event in vessels of S961 hyperglycemic rabbits, a crosstalk with other sources of ROS and their activation in the vessel wall is also likely. The lower levels of NO in hyperglycemia can be the result of scavenging by NADPH oxidase-derived ROS. Additionally, a shift in redox potential by ROS can promote eNOS glutathionylation and uncoupling. Thus, eNOS glutathionylation acts as a mechanism for amplification of ROS generation, exacerbating NO/redox imbalance in hyperglycemia.

To examine the putative mechanisms for eNOS uncoupling, we focused on eNOS glutathionylation as it is an enzymatically reversible mechanism (like phosphorylation) and is likely

to be involved in pathophysiological signaling, in particular in our model of relatively short-term hyperglycemia. It is plausible that increased redox stress by eNOS glutathionylation-mediated O<sub>2</sub><sup>•-</sup> generation may also lead to BH<sub>4</sub> depletion that can play a role in eNOS uncoupling in S961-induced hyperglycemia. Such a role might particularly be of more pathological significance over extended periods of hyperglycemia. Supportive evidence for a potential role of BH<sub>4</sub> in S961 hyperglycemia is provided by our observations in isolated cardiac myocytes where incubation of the myocytes with L-sepiapterin, a cell-permeable immediate precursor of BH<sub>4</sub> that is converted to BH<sub>4</sub> intracellularly via the pterin salvage pathway,<sup>37</sup> increased the electrogenic Na<sup>+</sup>-K<sup>+</sup> current in voltage clamped cardiomyocytes of rabbits with S961 hyperglycemia (unpublished data). This increase in pump current was abolished by L-N<sup>G</sup>-nitroarginine methyl ester, showing that stimulation was mediated by eNOS-derived NO production enhanced by ex vivo supplementation of BH<sub>4</sub>. In previous reports we have shown that NO generation from eNOS stimulates the Na<sup>+</sup>-K<sup>+</sup> pump,<sup>10,38</sup> and conditions that cause eNOS uncoupling inhibit the Na<sup>+</sup>-K<sup>+</sup> pump.<sup>24,39</sup> This



**Figure 6.** eNOS glutathionylation in vessels of diabetic humans and effects of β<sub>3</sub> AR stimulation in human endothelial cells and vascular tissue. A, Glutathione (GSH) and eNOS IB of eNOS IP from homogenates of the arteries from diabetic patients and their matched nondiabetic controls. There was a nonsignificant trend for increase in eNOS/eNOS co-immunoprecipitation in diabetics (bottom bands). The values for eNOS-GSS shown in the panel are the mean of densitometries normalized to the corresponding eNOS/eNOS bands. The median of the densitometries was 0.95 (IQR 0.8–1.0) in nondiabetics vs 1.87 (IQR 1.66–2.04) in diabetics. n=4. IP with a nonspecific IgG was used as negative control. B, The effect of CL (1 μmol/L, 37°C, 1 hour) on basal NO-sensitive DAF-FM fluorescence in HUVECs. The cell nuclei were counterstained with DAPI (blue). n=4. Cells from 2 to 3 randomly chosen areas of interest in each group were analyzed. C, Glutathione- and eNOS IB of eNOS IP from homogenates of the freshly harvested arteries from diabetic patients exposed to CL (1 μmol/L, 37°C, 1 hour) ex vivo. Mean densitometries are shown. The median of the densitometries was 1.0 (IQR 0.89–1.24) in –CL group vs 0.48 (IQR 0.36–0.66) in +CL group. n=4. IP with a nonspecific IgG was used as negative control. \*P<0.05 vs control. β<sub>3</sub> AR indicates β<sub>3</sub> adrenergic receptors; CL, CL316243; DAF-FM, 4-amino-5-methylamino-2',7'-difluorofluorescein; DAPI, 4',6-diamidino-2-phenylindole; DAPI; eNOS, endothelial nitric oxide synthase; GSS, glutathionylation; HUVECs, human umbilical vein endothelial cells; IB, immunoblot; IP, immunoprecipitate; IQR, interquartile range.

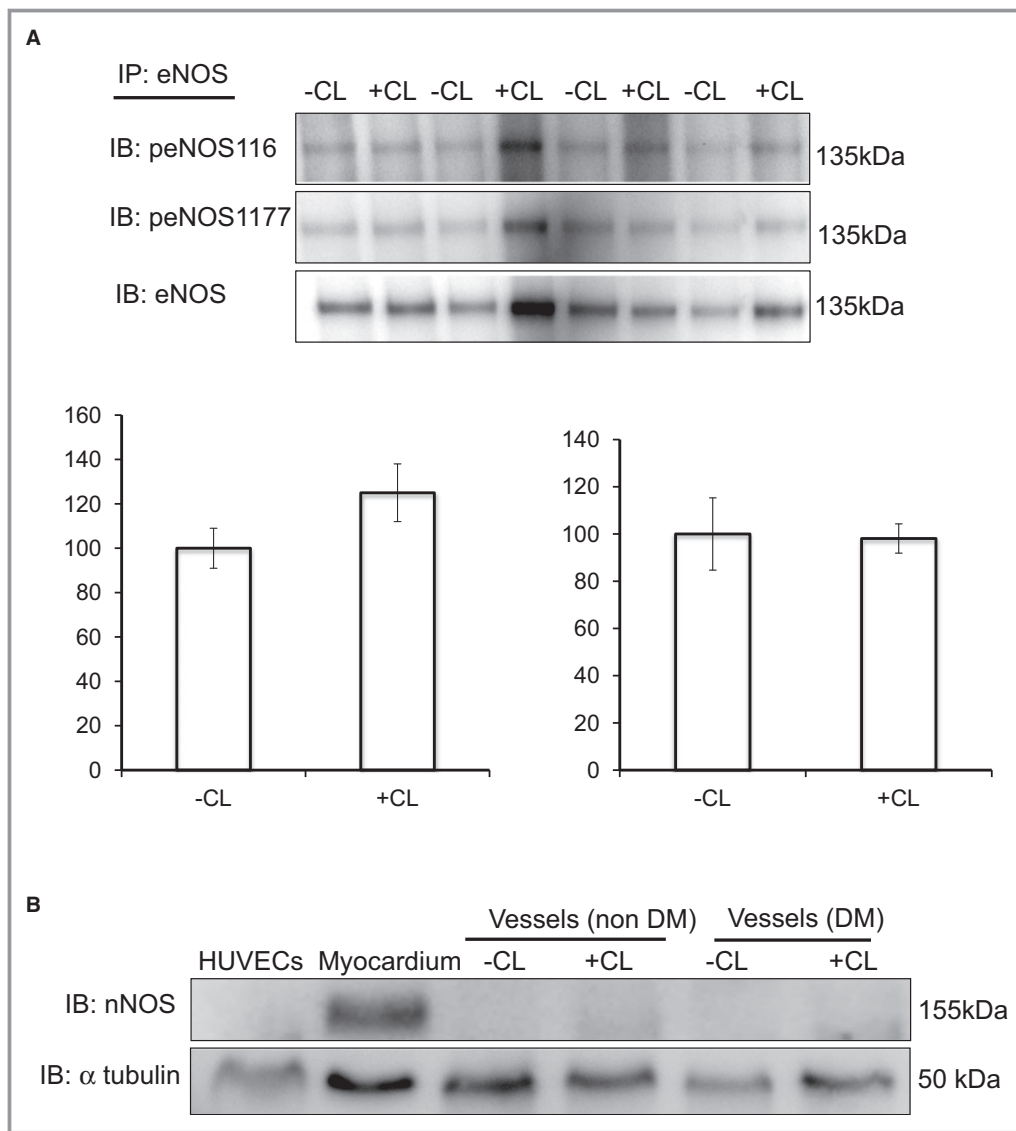


**Figure 7.** Effects of CL on eNOS phosphorylation in human endothelial cells, and expression of nNOS in human endothelial cells or vessels. A, Immunoblot (IB) of peNOS at serine 114 and 1177 residues from eNOS immunoprecipitate of HUVECs with (+CL) and without (–CL) exposure to CL (n=4). B, Immunoblots of nNOS in HUVECs, human myocardium (positive control), and arterial segments from diabetic (DM) and nondiabetic (non DM) patients exposed to CL ex vivo. CL indicates CL316243; eNOS, endothelial nitric oxide synthase; peNOS, phosphorylated endothelial nitric oxide synthase; HUVECs, human umbilical vein endothelial cells; IB, immunoblot; IP, immunoprecipitate; nNOS, neuronal nitric oxide synthase.

scheme shows a direct and physiologically important signaling interaction between these 2 important membrane biomolecules that colocalize in the structured membrane signaling microdomains<sup>40</sup> where changes in redox milieu are sensed by eNOS and transduced to regulation of the Na<sup>+</sup>-K<sup>+</sup> pump function via redox-dependent mechanisms. We have shown that eNOS glutathionylation is also increased in cardiac myocytes of S961 hyperglycemic rabbits and contributes to oxidative pump inhibition.<sup>25</sup> The effect of L-sepiapterin to stimulate Na<sup>+</sup>-K<sup>+</sup> pump from a basal inhibited state compared

to controls suggests that decreased BH<sub>4</sub> may coexist and play a role in eNOS uncoupling in the S961 model.

Reversal of glutathionylation of proteins (ie, de-glutathionylation) is catalyzed by Grx1. Grx1 is implicated in regulation of many intracellular processes related to homeostasis and stress response,<sup>26</sup> including redox-mediated regulation of eNOS function.<sup>41</sup> Despite its important roles, mechanisms regulating cellular activity of Grx1 are poorly understood. It has been proposed that association of Grx1 with scaffolding proteins (eg, caveolae in membrane lipid rafts) may regulate

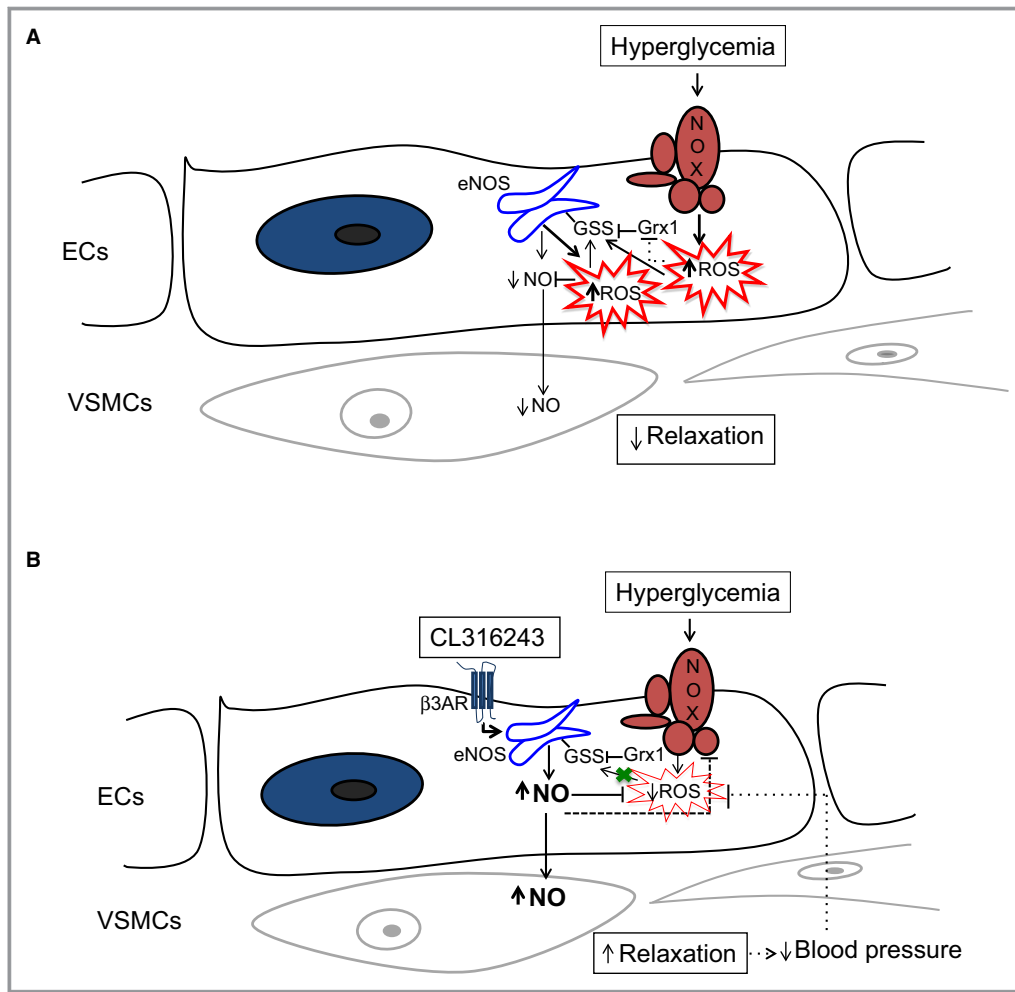


**Figure 8.** β<sub>3</sub> AR stimulation, redox- and NO-dependent signaling and endothelial function in hyperglycemia. A, NADPH oxidase (NOX) is activated in aorta of rabbits with S961-induced hyperglycemia, increasing the levels of ROS. ROS can directly scavenge and decrease NO levels, increase eNOS glutathionylation (eNOS-GSS) and, possibly, impair de-glutathionylation by affecting the activity of glutaredoxin-1 (Grx1) through yet unknown but likely redox-dependent mechanism(s)<sup>26</sup> (dashed line). Glutathionylation-mediated eNOS uncoupling results in eNOS-derived ROS generation, which might further increase eNOS-GSS and reduce NO bioavailability in endothelial cells (ECs) and impair relaxation of vascular smooth muscle cells (VSMCs). B, The β<sub>3</sub> AR agonist CL316243 (CL) increases NO. NO effect in reducing ROS by direct quenching may also decrease eNOS-derived ROS by reducing ROS-induced eNOS-GSS (green cross). Additionally, NO may decrease NOX activity (dashed line). An increase in Grx1/eNOS association by CL suggests enhanced eNOS de-glutathionylation by Grx1. These changes induced by CL culminate in enhanced vasodilatation, which may in turn reduce blood pressure (dotted arrow). A decrease in blood pressure per se may contribute to these beneficial changes (dotted line). β<sub>3</sub> AR indicates β<sub>3</sub> adrenergic receptors; eNOS, endothelial nitric oxide synthase; GSS, glutathionylation; ROS, reactive oxygen species.

Grx1 function, as the activity of the enzyme is thought to occur via an *encounter reaction*.<sup>26</sup> Consistent with this proposal, we show that Grx1 co-immunoprecipitates with eNOS in rabbit aorta. Interestingly, despite no change in the abundance of Grx1 in hyperglycemia, and an increase in glutathionylation of eNOS, we detected markedly lower signals for Grx1/eNOS co-immunoprecipitation in aorta of hyperglycemic rabbits. This suggests that interaction of Grx1 with its substrate (ie, glutathionylated cysteines) is not

determined by abundance of the substrate, but by other disease-related mechanisms. ROS and reactive nitrogen species reduce Grx1 activity<sup>41</sup>; therefore, it is likely that hyperglycemia may impair the enzyme function through redox-related mechanisms, leading to a decrease in de-glutathionylation and thereby increase in eNOS glutathionylation.

Infusion of CL restored NO levels in aorta of hyperglycemic rabbits. These effects of CL could be the result of less

quenching of NO by the decreased levels of ROS, a reduction in ROS-induced eNOS glutathionylation, and an increase in eNOS/Grx1 interaction promoting eNOS de-glutathionylation and recoupling. The effect of CL to decrease eNOS glutathionylation is in agreement with higher eNOS glutathionylation in the hearts of  $\beta_3$  AR<sup>-/-</sup> mice we have recently reported,<sup>25</sup> suggesting that both constitutive- and agonist-induced activation of the receptor is necessary to maintain eNOS in coupled state. In contrast to NO release by  $\beta_3$  AR stimulation, in vivo treatment with an external NO donor increases eNOS glutathionylation,<sup>42</sup> an effect that is consistent with NO donor-induced endothelial dysfunction. These differential effects are likely due to regulated endogenous NO generation via receptor-coupled pathway in the membrane signalosomes as opposed to general exposure of cells to uncontrolled levels by external NO donors. Although not examined, it is plausible that other antioxidant mechanisms in addition to the thiol reductase system are facilitated by treatment with CL, restoring NO levels in hyperglycemic rabbits. Since activation of insulin receptors is coupled to eNOS stimulation,<sup>17</sup> blockade of insulin receptor by S961 might have also contributed to reduced NO bioavailability in hyperglycemic rabbits. Because of the marked counter-regulatory increase in insulin levels, slightly higher affinity of insulin in binding to insulin receptor compared to S961 and competitive nature of antagonism of the insulin receptor by S961 shown previously,<sup>18</sup> the blockade of insulin receptor-coupled signaling in S961 hyperglycemia is likely relative and not absolute. Moreover, near-complete restoration of NO bioavailability by CL co-administered with S961 suggests that insulin-receptor-coupled eNOS activation probably did not significantly contribute to lower NO levels in S961 hyperglycemic rabbits.

The effect of CL in decreasing  $O_2^{\bullet-}$  levels is the result of recoupling of eNOS as well as a decrease in NADPH oxidase activation as suggested by reduction in p47<sup>phox</sup>/eNOS co-immunoprecipitation. NO can directly inhibit NADPH oxidase by nitrosylation of p47<sup>phox</sup>, although this does not affect its membrane translocation.<sup>43</sup> Other putative mechanisms are oxidative modification of cysteines on p47<sup>phox</sup>, important in downregulation of the enzyme,<sup>44</sup> and, as recently reported by our group in cardiac myocytes, by NO signaling-mediated dephosphorylation and inactivation of p47<sup>phox</sup> subunit by protein phosphatase 2A.<sup>38</sup>

CL decreased hyperglycemia-induced glutathionylation of  $\beta_1$  Na<sup>+</sup>-K<sup>+</sup> pump subunit, a redox modification that inhibits the pump,<sup>23,24</sup> and enhanced pump activity as implied by increased K<sup>+</sup>-induced vasorelaxation. This should largely reflect the signal from vascular smooth muscle cells as the media layer constitutes the major part of the vascular wall. We have previously shown that AngII inhibits the pump in vascular smooth muscle cells via an NADPH oxidase-dependent increase in  $\beta_1$  subunit glutathionylation.<sup>23</sup> CL

restored NO bioavailability in aorta and we have shown that  $\beta_3$  AR stimulation in cardiac myocytes decreases glutathionylation of the Na<sup>+</sup>-K<sup>+</sup> pump via NO-dependent mechanisms in vitro<sup>10</sup> and in vivo in hyperglycemia.<sup>25</sup> A reduction in NO bioavailability in endothelial cells of hyperglycemic rabbits diffusing into the subjacent vascular smooth muscle cells is a likely mechanism by which glutathionylation of  $\beta_1$  Na<sup>+</sup>-K<sup>+</sup> subunit is increased, and reversed by re-establishment of NO levels by  $\beta_3$  AR agonism. Moreover, similar to what we observed with eNOS, CL also enhanced co-immunoprecipitation of Grx1 with  $\beta_1$  subunit, which may indicate facilitation of  $\beta_1$  subunit de-glutathionylation. Given the central role of the pump in regulation of cellular homeostasis, enhancement of Na<sup>+</sup>-K<sup>+</sup> pump function by CL is expected to contribute to improved vascular function in diabetes.<sup>23</sup>

Vasodilatory effects of nebivolol, a highly selective  $\beta_1$  AR blocker, in arteries of normal animals have been reported to occur via  $\beta_3$  AR agonism.<sup>45</sup> However, nebivolol has a weak affinity for human  $\beta_3$  AR and elicited no receptor-coupled response in Chinese hamster ovary cells expressing  $\beta_3$  ARs.<sup>46</sup> Using CL, with its high selectivity for  $\beta_3$  ARs<sup>47</sup> and high efficacy,<sup>48</sup> we show potent, novel antioxidant and vasoprotective effects of  $\beta_3$  AR stimulation in hyperglycemia. Glutathionylation of eNOS has been reported in STZ-induced diabetes.<sup>49</sup> Our recent report of eNOS glutathionylation as a critical switch in AngII-induced endothelial dysfunction<sup>7</sup> suggested a mechanistic rationale for renin-angiotensin system-mediated diabetes-induced complications.<sup>17</sup> The current study shows the central role of this oxidative modification of eNOS in the pathophysiology of vascular dysfunction, its cellular regulatory mechanisms, a novel therapy that modulates it in experimental hyperglycemia, and provides supportive evidence for potential significance of this pathway in human diabetes.

Early rodent models of diabetes and obesity showed promising effects of  $\beta_3$  AR agonists on glycemic control and weight loss. However, subsequent human trials were disappointing, at least in part due to major differences in pharmacology of the agonists between rodent and human receptors, differences in tissue-dependent expression levels, poor selectivity of the agonists for  $\beta_3$ - versus  $\beta_1/\beta_2$  ARs, and unsatisfactory oral bioavailability and pharmacokinetic properties.<sup>50</sup> Problems with pharmacological properties have been overcome<sup>51</sup> and one compound, Mirabegron, is now in clinical use for overactive bladder syndrome.<sup>52</sup> Evidence from experimental models that support beneficial effects of  $\beta_3$  AR agonists in failing heart is accumulating,<sup>10,11,52-54</sup> and a phase 2 first-in-human clinical trial of Mirabegron in chronic heart failure has recently been completed.<sup>55</sup> The protective effects of a  $\beta_3$  AR agonist in hyperglycemia we report suggest that they can be potentially useful in treating the vascular dysfunction and cardiovascular complications of diabetes. We believe such a use deserves further clinical investigation.

## Acknowledgments

We thank Lauge Schaeffer (Novo Nordisk, Denmark) for the generous supply of S961 peptide.

## Sources of Funding

The project was supported by a project grant from Australian National Health & Medical Research Council (NHMRC grant 633252). Karimi Galougahi was supported by a Heart Research Australia Scholarship and Lucy Falkiner Fellowship from University of Sydney Medical School Foundation, Liu by a Heart Foundation Fellowship (PF 12S 6924), and Figtree by University of Sydney Medical School Foundation and a co-funded NHMRC/Heart Foundation Fellowship.

## Disclosures

None.

## References

- Giacco F, Brownlee M. Oxidative stress and diabetic complications. *Circ Res*. 2010;107:1058–1070.
- Guzik TJ, Harrison DG. Vascular NADPH oxidases as drug targets for novel antioxidant strategies. *Drug Discovery Today*. 2006;11:524–533.
- Zimmet JM, Hare JM. Nitroso-redox interactions in the cardiovascular system. *Circulation*. 2006;114:1531–1544.
- Burgoyne JR, Mongue-Din H, Eaton P, Shah AM. Redox signaling in cardiac physiology and pathology. *Circ Res*. 2012;111:1091–1106.
- Majkova Z, Toborek M, Hennig B. The role of caveolae in endothelial cell dysfunction with a focus on nutrition and environmental toxicants. *J Cell Mol Med*. 2010;14:2359–2370.
- Munzel T, Gori T, Bruno RM, Taddei S. Is oxidative stress a therapeutic target in cardiovascular disease? *Eur Heart J*. 2010;31:2741–2748.
- Galougahi KK, Liu CC, Gentile C, Kok C, Nunez A, Garcia A, Fry NA, Davies MJ, Hawkins CL, Rasmussen HH, Figtree GA. Glutathionylation mediates angiotensin II-induced eNOS uncoupling, amplifying NADPH oxidase-dependent endothelial dysfunction. *J Am Heart Assoc*. 2014;3:e000731 doi: 10.1161/JAHA.113.000731.
- Dessy C, Moniotte S, Ghisdal P, Havaux X, Noirhomme P, Balligand JL. Endothelial beta3-adrenoceptors mediate vasorelaxation of human coronary microarteries through nitric oxide and endothelium-dependent hyperpolarization. *Circulation*. 2004;110:948–954.
- Sato M, Hutchinson DS, Halls ML, Furness SG, Bengtsson T, Evans BA, Summers RJ. Interaction with caveolin-1 modulates G protein coupling of mouse beta3-adrenoceptor. *J Biol Chem*. 2012;287:20674–20688.
- Bundgaard H, Liu C-C, Garcia A, Hamilton EJ, Huang Y, Chia KKM, Hunyor SN, Figtree GA, Rasmussen HH. β3 adrenergic stimulation of the cardiac Na<sup>+</sup>-K<sup>+</sup> pump by reversal of an inhibitory oxidative modification. *Circulation*. 2010;122:2699–2708.
- Galougahi KK, Liu CC, Bundgaard H, Rasmussen HH. beta-Adrenergic regulation of the cardiac Na<sup>+</sup>-K<sup>+</sup> ATPase mediated by oxidative signaling. *Trends Cardiovasc Med*. 2012;22:83–87.
- Cai T, Wang H, Chen Y, Liu L, Gunning WT, Quintas LE, Xie ZJ. Regulation of caveolin-1 membrane trafficking by the Na/K-ATPase. *J Cell Biol*. 2008;182:1153–1169.
- Gallooly MM, Mieyal JJ. Mechanisms of reversible protein glutathionylation in redox signaling and oxidative stress. *Curr Opin Pharmacol*. 2007;7:381–391.
- Chen CA, Wang TY, Varadharaj S, Reyes LA, Hemann C, Talukder MA, Chen YR, Druhan LJ, Zweier JL. S-glutathionylation uncouples eNOS and regulates its cellular and vascular function. *Nature*. 2010;468:1115–1118.
- Crabtree MJ, Brixey R, Batchelor H, Hale AB, Channon KM. Integrated redox sensor and effector functions for tetrahydrobiopterin- and glutathionylation-dependent endothelial nitric-oxide synthase uncoupling. *J Biol Chem*. 2013;288:561–569.
- Paneni F, Beckman JA, Creager MA, Cosentino F. Diabetes and vascular disease: pathophysiology, clinical consequences, and medical therapy: part I. *Eur Heart J*. 2013;34:2436–2443.
- Kim JA, Montagnani M, Koh KK, Quon MJ. Reciprocal relationships between insulin resistance and endothelial dysfunction: molecular and pathophysiological mechanisms. *Circulation*. 2006;113:1888–1904.
- Schaffer L, Brand CL, Hansen BF, Ribel U, Shaw AC, Slaaby R, Sturis J. A novel high-affinity peptide antagonist to the insulin receptor. *Biochem Biophys Res Commun*. 2008;376:380–383.
- Audigane L, Kerfant B-G, El Harchi A, Lorenzen-Schmidt I, Toumaniantz G, Cantereau A, Potreau D, Charpentier F, Noireaud J, Gauthier C. Rabbit, a relevant model for the study of cardiac β<sub>3</sub>-adrenoceptors. *Exp Physiol*. 2009;94:400–411.
- Kleschyov AL, Mollnau H, Oelze M, Meinertz T, Huang Y, Harrison DG, Munzel T. Spin trapping of vascular nitric oxide using colloid Fe(II)-diethyldithiocarbamate. *Biochem Biophys Res Commun*. 2000;275:672–677.
- Zielonka J, Vasquez-Vivar J, Kalyanaraman B. Detection of 2-hydroxyethidium in cellular systems: a unique marker product of superoxide and hydroethidine. *Nat Protoc*. 2008;3:8–21.
- Webb RC, Bohr DF. Potassium-induced relaxation as an indicator of Na<sup>+</sup>-K<sup>+</sup> ATPase activity in vascular smooth muscle. *Blood Vessels*. 1978;15:198–207.
- Liu C-C, Karimi Galougahi K, Weisbrod RM, Hansen T, Ravaie R, Nunez A, Liu YB, Fry N, Garcia A, Hamilton EJ, Sweadner KJ, Cohen RA, Figtree GA. Oxidative inhibition of the vascular Na<sup>+</sup>-K<sup>+</sup> pump via NADPH oxidase-dependent β1-subunit glutathionylation: implications for angiotensin II-induced vascular dysfunction. *Free Radic Biol Med*. 2013;65:563–572.
- Figtree GA, Liu CC, Bibert S, Hamilton EJ, Garcia A, White CN, Chia KKM, Cornelius F, Geering K, Rasmussen HH. Reversible oxidative modification: a key mechanism of Na<sup>+</sup>-K<sup>+</sup> pump regulation. *Circ Res*. 2009;105:185–193.
- Karimi Galougahi K, Liu CC, Garcia A, Fry NA, Hamilton EJ, Figtree GA, Rasmussen HH. beta3-Adrenoceptor activation relieves oxidative inhibition of the cardiac Na<sup>+</sup>-K<sup>+</sup> pump in hyperglycemia induced by insulin receptor blockade. *Am J Physiol Cell Physiol*. 2015;309:C286–C295.
- Gallooly MM, Starke DW, Mieyal JJ. Mechanistic and kinetic details of catalysis of thiol-disulfide exchange by glutaredoxins and potential mechanisms of regulation. *Antioxid Redox Signal*. 2009;11:1059–1081.
- Niu X, Watts VL, Cingolani OH, Sivakumaran V, Leyton-Mange JS, Ellis CL, Miller KL, Vandegaer K, Bedja D, Gabrielson KL, Paolucci N, Kass DA, Barouch LA. Cardioprotective effect of beta-3 adrenergic receptor agonism: role of neuronal nitric oxide synthase. *J Am Coll Cardiol*. 2012;59:1979–1987.
- Watts VL, Sepulveda FM, Cingolani OH, Ho AS, Niu X, Kim R, Miller KL, Vandegaer K, Bedja D, Gabrielson KL, Rameau G, O'Rourke B, Kass DA, Barouch LA. Anti-hypertrophic and anti-oxidant effect of beta3-adrenergic stimulation in myocytes requires differential neuronal NOS phosphorylation. *J Mol Cell Cardiol*. 2013;62:8–17.
- Chakrabarti S, Chan CK, Jiang Y, Davidge ST. Neuronal nitric oxide synthase regulates endothelial inflammation. *J Leukoc Biol*. 2012;91:947–956.
- Bugger H, Abel ED. Rodent models of diabetic cardiomyopathy. *Dis Model Mech*. 2009;2:454–466.
- Szkudelski T. The mechanism of alloxan and streptozotocin action in B cells of the rat pancreas. *Physiol Res*. 2001;50:537–546.
- Sakurai K, Katoh M, Fujimoto Y. Alloxan-induced mitochondrial permeability transition triggered by calcium, thiol oxidation, and matrix ATP. *J Biol Chem*. 2001;276:26942–26946.
- Black SM. β3-Adrenoceptor, glutathionylation, and diabetic cardiomyopathy. Focus on “beta3 adrenoceptor activation relieves oxidative inhibition of the cardiac Na<sup>+</sup>-K<sup>+</sup> pump in hyperglycemia induced by insulin receptor blockade”. *Am J Physiol Cell Physiol*. 2015;309:C283–285.
- Gao L, Mann GE. Vascular NAD(P)H oxidase activation in diabetes: a double-edged sword in redox signalling. *Cardiovasc Res*. 2009;82:9–20.
- Guzik TJ, Mussa S, Gastaldi D, Sadowski J, Ratnatunga C, Pillai R, Channon KM. Mechanisms of increased vascular superoxide production in human diabetes mellitus: role of NAD(P)H oxidase and endothelial nitric oxide synthase. *Circulation*. 2002;105:1656–1662.
- Youn JY, Siu KL, Li Q, Harrison DG, Cai H. Oxidase interactions in cardiovascular disease. In: Ismail LAHER, ed. *Systems Biology of Free Radicals and Antioxidants*. Berlin, Heidelberg: Springer; 2014:849–876.
- Mayer B, Werner ER. In search of a function for tetrahydrobiopterin in the biosynthesis of nitric oxide. *Naunyn Schmiedebergs Arch Pharmacol*. 1995;351:453–463.

38. Chia KK, Liu CC, Hamilton EJ, Garcia A, Fry NA, Hannam W, Figtree GA, Rasmussen HH. Stimulation of the cardiac myocyte Na<sup>+</sup>-K<sup>+</sup> pump due to reversal of its constitutive oxidative inhibition. *Am J Physiol Cell Physiol*. 2015;309:C239–C250.
39. White CN, Hamilton EJ, Garcia A, Wang D, Chia KKM, Figtree GA, Rasmussen HH. Opposing effects of coupled and uncoupled NOS activity on the Na<sup>+</sup>-K<sup>+</sup> pump in cardiac myocytes. *Am J Physiol Cell Physiol*. 2008;294:C572–C578.
40. Figtree GA, Keyvan Karimi G, Liu CC, Rasmussen HH. Oxidative regulation of the Na(+)-K(+) pump in the cardiovascular system. *Free Radic Biol Med*. 2012;53:2263–2268.
41. Chen CA, De Pascali F, Basye A, Hemann C, Zweier JL. Redox modulation of endothelial nitric oxide synthase by glutaredoxin-1 through reversible oxidative post-translational modification. *Biochemistry*. 2013;52:6712–6723.
42. Knorr M, Hausding M, Kroller-Schuhmacher S, Steven S, Oelze M, Heeren T, Scholz A, Gori T, Wenzel P, Schulz E, Daiber A, Munzel T. Nitroglycerin-induced endothelial dysfunction and tolerance involve adverse phosphorylation and S-glutathionylation of endothelial nitric oxide synthase: beneficial effects of therapy with the AT1 receptor blocker telmisartan. *Arterioscler Thromb Vasc Biol*. 2011;31:2223–2231.
43. Selemidis S, Dusting GJ, Peshavariya H, Kemp-Harper BK, Drummond GR. Nitric oxide suppresses NADPH oxidase-dependent superoxide production by S-nitrosylation in human endothelial cells. *Cardiovasc Res*. 2007;75:349–358.
44. Babior BM. The activity of leukocyte NADPH oxidase: regulation by p47PHOX cysteine and serine residues. *Antioxid Redox Signal*. 2002;4:35–38.
45. Feng MG, Prieto MC, Navar LG. Nebivolol-induced vasodilation of renal afferent arterioles involves beta3-adrenergic receptor and nitric oxide synthase activation. *Am J Physiol Renal Physiol*. 2012;303:F775–F782.
46. Baker JG. The selectivity of beta-adrenoceptor agonists at human beta1-, beta2- and beta3-adrenoceptors. *Br J Pharmacol*. 2010;160:1048–1061.
47. Baker JG. The selectivity of beta-adrenoceptor antagonists at the human beta1, beta2 and beta3 adrenoceptors. *Br J Pharmacol*. 2005;144:317–322.
48. Sato M, Horinouchi T, Hutchinson DS, Evans BA, Summers RJ. Ligand-directed signaling at the beta3-adrenoceptor produced by 3-(2-ethylphenoxy)-1-[(1, S)-1,2,3,4-tetrahydronaph-1-ylamino]-2S-2-propanol oxalate (SR59230A) relative to receptor agonists. *Mol Pharmacol*. 2007;72:1359–1368.
49. Schuhmacher S, Oelze M, Bollmann F, Kleinert H, Otto C, Heeren T, Steven S, Hausding M, Knorr M, Pautz A, Reifenberg K, Schulz E, Gori T, Wenzel P, Munzel T, Daiber A. Vascular dysfunction in experimental diabetes is improved by pentaerythrityl tetranitrate but not isosorbide-5-mononitrate therapy. *Diabetes*. 2011;60:2608–2616.
50. de Souza CJ, Burkey BF. Beta 3-adrenoceptor agonists as anti-diabetic and anti-obesity drugs in humans. *Curr Pharm Des*. 2001;7:1433–1449.
51. Arch JR. Challenges in beta(3)-adrenoceptor agonist drug development. *Ther Adv Endocrinol Metab*. 2011;2:59–64.
52. Rasmussen HH, Figtree GA, Krum H, Bundgaard H. Treatment of heart failure with β<sub>3</sub>-receptor agonists. *Curr Opin Investig Drugs*. 2009;10:955–962.
53. Kulandavelu S, Hare JM. Alterations in beta3-adrenergic cardiac innervation and nitric oxide signaling in heart failure. *J Am Coll Cardiol*. 2012;59:1988–1990.
54. Fry NA, Garcia A, Karimi Galougahi K, Liu CC, Hamilton EJ, McLachlan CS, Figtree GA. Treatment with a beta3 adrenergic receptor agonist in heart failure reverses an oxidative modification and inhibition of the Na<sup>+</sup>-K<sup>+</sup> pump in cardiac myocytes and improves pulmonary congestion. *Circulation*. 2013;128:A17142.
55. National Library of Medicine (US). Beta 3 agonist treatment in heart failure (Beat-HF) (Online). Available at: <http://clinicaltrials.gov/show/NCT01876433>. Accessed August 22, 2015.